Synthesis, Characterization and Applications of Nickel loaded SBA-15

Neel Kamal Kalita[a], and Jatindra Natha Ganguli[b*]
[a]State Public Health Laboratory, Guwahati, Assam, 781021
[b] Department of Chemistry, University of Science and Technology, Meghalaya.793101
*Corresponding author's Email: gangjn16@gmail.com

Abstract: In the present study, we report the modification of SBA-15 with nickel incorporation by post synthetic treatments and its catalytic application. The synthesized SBA-15 materials were characterized by Nitrogen adsorption-desorption studies, XRD and TEM. The nickel loaded SBA-15 materials were successfully used to catalyze the model reaction of reduction of 4-nitrophenol to 4-aminophenol using sodium borohydride.

***Keywords**: SBA-15, Ni-SBA-15, Mesoporous, Catalysis.*

Introduction

SBA-15 as well as functionalized and metal modified SBA-15 find widespread applications in the fields of catalysis [1-4] , adsorption[5,6], drug delivery[7,8] etc. In the field of catalysis, a lot of attention has been concentrated on application of SBA-15 as noble metal support for catalysis. H. Wang et al. [9] reported synthesis of highly dispersed palladium nanoparticles within the uniform channels of SBA-15 via a glow discharge plasma reduction treatment which showed good activity for CO oxidation. Silver nanoparticles within the pore channels of formaldehyde grafted mesoporous silica SBA-15 were synthesized by D. Lin and co-workers for applications in hydrogen peroxide sensing by the Ag-mSBA-15 modified electrode [10]. Highly dispersed Pt nanoparticles on modified mesoporous Al-SBA-15 were also prepared by a solid state impregnation (SSI) methodology. Various metals can be incorporated into the meso-channels of SBA-15 by wetness impregnation method in a post synthetic route for the modification of pure SBA-15 [11-13]. Here we explore into the simple method of wetness impregnation for preparing Nickel loaded SBA-15 and the potential applications in catalysis [13,14].

Materials and methods

Poly (ethylene glycol) block poly (propylene glycol) block poly (ethylene glycol), P123, ($EO_{20}PO_{70}EO_{20}$, MW = 5800 g/mol) and Nickel Nitrate were purchased from Aldrich. Tetraethylorthosilicate (TEOS) was bought from Merck and used as the silica source. The materials were used without further purification or any modification.

Synthesis of Ni-SBA-15

Firstly, the SBA-15 materials were prepared following the method of Stucky *et al*[15]. In a typical synthetic procedure, 4g of the surfactant Pluronic P123 were dissolved in 140mL of 2N hydrochloric acid by continuous stirring using a mechanical stirrer in a Teflon beaker. The temperature of the mixture was then kept a 40 °C and 8.6g of Tetraethylorthosilicate (TEOS) was added dropwise to the mixture while stirring was continued. The mixtures was stirred for 12 hours and then aged at 100 °C for another 48 hours in a Teflon lined autoclave. Then the product was filtered, washed with distilled water and ethanol. The products were then dried at 80 °C in an air oven for 12 hours. In the final step, the organic template was removed from the silica materials by calcination at 550 °C for 5 hours, before attaining the calcination temperature, the SBA-15 was heated at a heating rate of 3 °C per minute to 550 °C. The final product was a pure white powder and the powder is designated as SBA-15. Then the nickel loaded SBA-15 materials were synthesized via post synthetic impregnation method [16,18]. In this method,

Ni-SBA-15 samples were prepared by incipient wetness impregnation of mesoporous SBA-15 support with the corresponding aqueous metal nitrate precursor solutions. In a typical synthesis, 0.5 g SBA-15 was mixed with 25 mL aqueous solution containing nickel nitrate [$Ni(NO_3)_2.6H_2O$, 0.1 M] under stirring at 60 °C until dryness, and then drying at 100 °C overnight. The dried material was finally calcined at 550 °C for 4.0 h under air at a heating rate of 5 °C per minute.

Characterization of Ni-SBA-15

Small angle XRD spectra were recorded on a Rigaku x-ray diffractometer for 2θ values from 0.5-10° using Cu-Kα source (λ = 1.54 Å). Wide angle X-Ray Diffraction (XRD) patterns were recorded using a Bruker D8 Advance diffractometer operating at a voltage of 40 kV and a current of 40 mA with Cu Kα radiation of wavelength 0.15406 nm. The nitrogen adsorption-desorption isotherms were measured using Micromeritics Tristar 3000 instrument. Before adsorption, the samples were degassed at 300 °C for 3 h. The method of Barrett, Joyner and Halenda (BJH) [19] was used for the mesopore size distributions from the experimental isotherms. High resolution Transmission Electron Micrographs (TEM) were captured with JEOL JEM 2100 TEM instrument operated at 200 kV. Ethanolic suspension of the samples were prepared on dry carbon coated Cu-grid.

Catalytic study

To test the catalytic activity of the synthesized Ni-SBA-15 materials were used as catalyst in the reduction reaction of 4-nitrophenol to 4-aminophenol by $NaBH_4$. For kinetic study of the reaction, the absorbance of corresponding to 4-nitrophenolate anion (λ_{max}= 400nm) was monitored at different time intervals. The reduction reaction of 4-nitropheol to 4-aminophenol (Scheme 1) has become academically as well as technologically important[20].

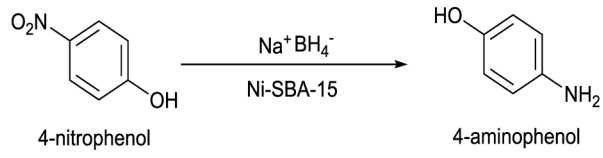

Scheme 1 Reduction of 4-NP to 4-AP in presence of catalyst

In this study, 1.5 mmol of 4-nitrophenol was mixed with 20 mmol Sodium borohydride in the presence of 10 mg catalyst per 50 mL of reaction mixture. During the reaction, the absorption peak of 4-nitrophenol undergoes a red shift from 317 to 400 nm (due to 4-nitrophenolate ion) immediately upon the addition of aqueous solution of $NaBH_4$, corresponding to a significant change in solution color from light yellow to yellow–green. Thus the course of the reaction can easily be monitored by recording the UV-Visible spectra of the reaction mixture at different time intervals.

Results and Discussion

X-Ray diffraction analysis

The low angle XRD patterns (Fig. 1) of the Ni-SBA-15 materials show similar peaks as seen in SBA-15. A strong peak around 2 theta value 1.03° can be indexed to the (100) reflection. Two more weak peaks can be indexed to (110) and (200) reflections. These peaks are characteristic of the of a 2D hexagonal structure *P6mm* symmetry of the mesoporous materials[21].

The wide angle powder XRD patterns (Fig. 2) of the Nickel loaded SBA-15 exhibited no recognizable specific diffraction peak of the nickel species. It was similar to pristine SBA-15 which was used as the mesoporous support. These results may be because nickel was so finely incorporated into the surface of the mesopore of the Ni-SBA-15 that it could not

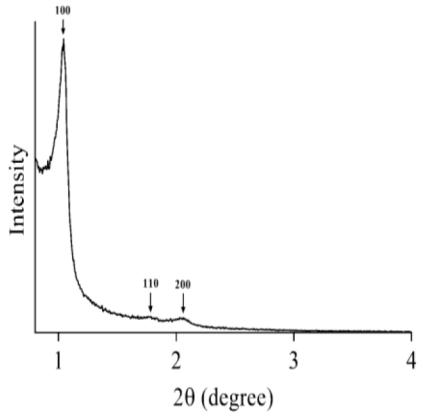

Fig. 1 Low angle powder XRD patterns of Ni-SBA-15

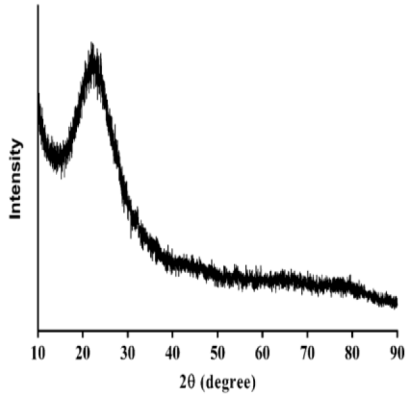

Fig. 2 Wide angle XRD patterns of Ni-SBA-15

form a crystalline structure[22]. The non-existence of characteristic peak representing crystalline nickel species may also be due to low loading amount of nickel into the mesoporous support[23].

All samples also show a broad silica peak around 2 theta value of 23° indicating an overall low degree of crystallization of the silica materials. The unit cell characteristics calculated from low angle XRD are tabulated below

Table 1 Unit cell characteristics of Ni-SBA-15

Miller Indices (*hkl*)	**2θ°**	**d-Value (Å)**	**Unit cell parameter a_0 (Å)**
100	1.03	85.7	98.96
110	1.79	49.31	
200	2.06	42.85	

Nitrogen adsorption desorption studies

The nitrogen adsorption-desorption isotherms were obtained following similar procedure as explained in case of SBA-15. The isotherm obtained is a type IV isotherm with combined H1 and and H3 hysteresis characteristics[24]. The isotherm is similar to mesoporous silica but with some characteristics of closed pore structure is evident from the ink-bottle type isotherm appearance[25].

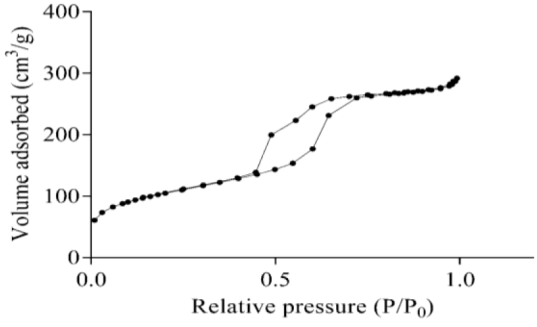

Fig. 3 Nitrogen adsorption desorption isotherm of Ni-SBA-15

The surface area of the materials were calculated using the BET method and the external surface area, micropore volume and micropore surface area were calculated using the correlation of *t*-Harkins and Jura plot (*t*-plot method)[26,27].

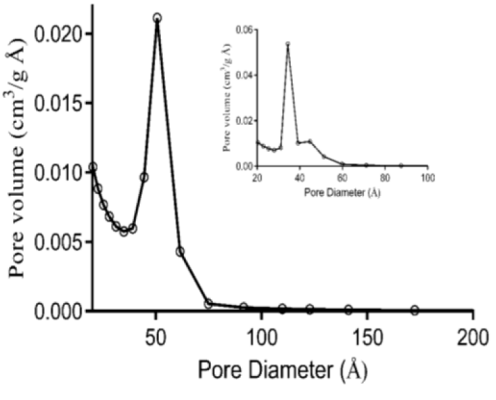

Fig. 4 Pore size distribution of Ni-SBA-15 of the adsorption branch; inset-desorption branch

The pore size distribution was calculated by BJH method using the desorption branch[28,29]

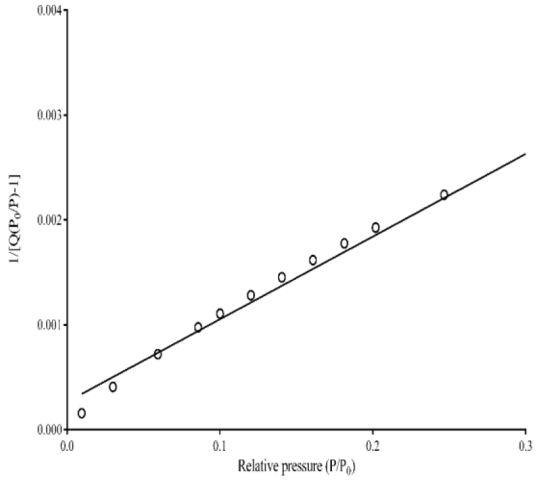

Fig. 5 BET plot of Ni-SBA-15

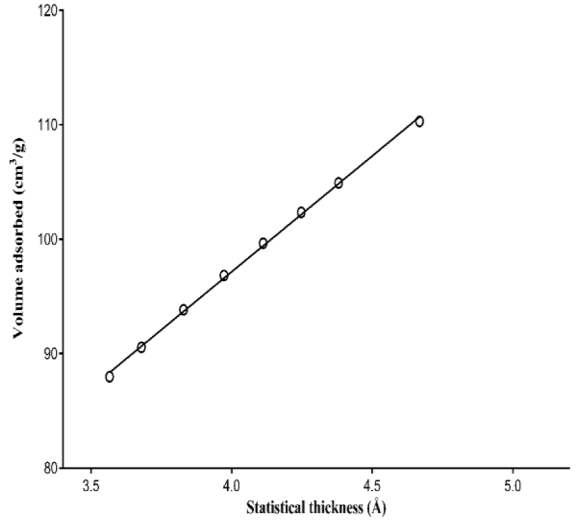

Fig. 6 Representative t-plot of Ni-SBA-15 in the thickness range 3.5-5Å

.

Table 2 Textural properties of Ni-SBA-15

BET surface area	534.89 m^2/g
External surface area	312.07 m^2/g
Micropore surface area	222.82 m^2/g
Micropore volume	0.02499 cm^3/g
Single point total pore volume (at $P/P_0 = 0.99286$)	0.4516 cm^3/g
BJH average pore size (desorption branch)	34.37 Å
BJH average pore size (adsorption branch)	50.77 Å
Pore wall thickness (from desorption pore size and a_0)	64.59 Å

The nitrogen-desorption experiments of Ni-SBA-15 shows Type IV isotherm with H3 type hysteresis *Fig.* . The BET method yielded lower total surface area than the pristine SBA-15 materials but still relatively high total surface area suitable for catalytic applications. From the t-plot analysis, it can be concluded that the materials contain micropores. The

slope of the fitted t-plot (*Fig.*) was used to calculate the external surface area and the intercept gave the micropore volume.

Transmission Electron Microscopy

The transmission electron micrographs of Ni-SBA-15 show hexagonal pore symmetry and confirm that the modified SBA-15 materials possess ordered one-dimensional pore structure similar to that of the pure SBA-15. However, a decrease in structural ordering from SBA-15 to Ni-SBA-15 can be observed from the images. The SAED patterns are typical of amorphous materials which may be due to very finely dispersed nickel in the silica matrix with low amount of loading.

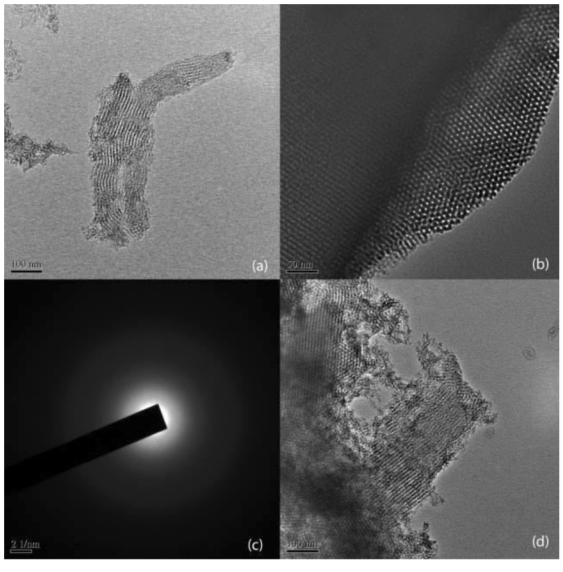

Fig. 7 Transmission Electron Microscopy images of Ni-SBA-15

Catalytic reduction of 4-nitrophenol

In the absence of the catalyst, peak at 400 nm remained unaltered for a long duration, indicating the inability of the strong reducing agent $NaBH_4$ alone to reduce 4-nitrophenolate ion even though the reaction medium contains the electron donor (BH_4^-) and proton source (H_2O). As suggested by Zhang *et al.*[30], the catalyst brings down the kinetic barrier created due to mutual repulsion between both negatively charged p-nitrophenolate ion and BH_4^- ion. Once the catalyst was added, there was a successive decrease in absorption peak at 400 nm corresponding to reduction of 4-nitrophenolate species.

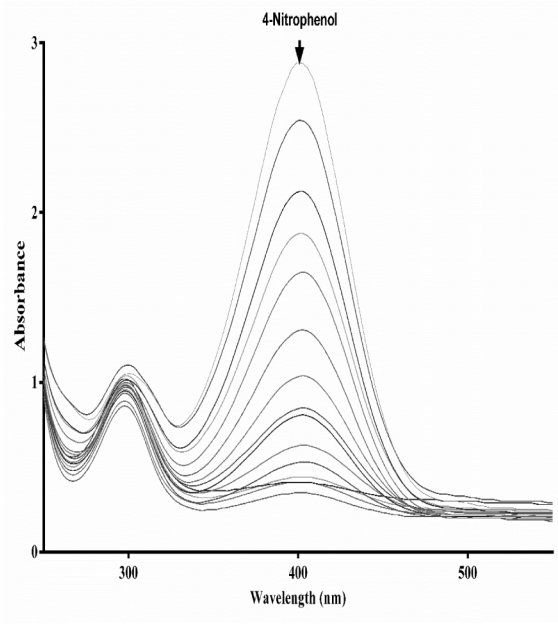

Fig. 8 UV-Visible spectra showing reduction of 4-NP.

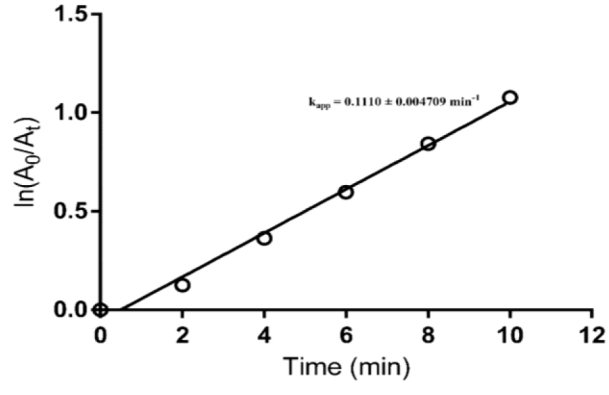

Fig. 9 Pseudo first order kinetics linear fit plot

In general, the mechanism for the heterogeneous catalysis reactions are studied using the classical Langmuir-Hinshelwood equation which is based on the reaction between the chemisorbed species on the surface of the catalyst and the same mechanism has been accepted to explain a majority of surface catalytic reactions both experimentally and theoretically[31]. We

thus employed the Langmuir-Hinshelwood mechanism considering that the reaction proceeds by encounter between the chemisorbed atoms on the surface of the catalyst and the substrate molecules[32]. The rate equation is used in the form[33]:

$$-\frac{dC}{dt} = \frac{k_{L-H}K_{ads}C}{1+K_{ads}C} \qquad (1)$$

On integrating Eq.1, pseudo-first-order reaction $K_{ads}C$ is very small compared to 1 in the denominator of Eq.1, so it is simplified and integrated to be:

$$\ln\left(\frac{C_0}{C_t}\right) = k_{L-H}K_{ads}t = k_{app}t \qquad (2)$$

Where, $k_{L-H}K_{ads}=k_{app}$, is the pseudo-first order reaction rate constant. The pseudo-first order reaction rate may be assumed to be proportional to the accessible surface area of the catalyst[32]. The concentrations C_0 and C_t have their equivalents in terms of the absorbance of the solution; they are noted A_0 and A_t respectively, and absorbance values were measured at a fixed wavelength (λ) at fixed time intervals, t. Therefore, for constant catalyst concentration and uniform accessible surface area by the reactants, a plot of $\ln(A_0/A_t)$ as a function of time results in a straight line whose slope is defined by the pseudo-first order rate constant *k* of the catalytic reactions.

The reaction between 4-NP and $NaBH_4$ has been used widely for investigating the catalytic activity of metal nanostructures owing to two important properties viz., the reaction does not occur without a catalyst and the catalyzed reaction can be monitored easily using UV-Visible spectrophotometric method (Fig. 8). As the initial concentration of $NaBH_4$ was very high and it remained constant throughout the reaction, we have considered that this catalytic reaction follows pseudo first order kinetics (Fig. 9) with apparent rate constant 0.1110±0.0047 min^{-1}.

Conclusions

We have successfully incorporated Nickel into the meso-channels of SBA-15 by post synthetic route. All the synthesized materials have high surface area and thus have potential catalytic activity. All materials also have micropore surface area confirmed by the t-plot method. Ni-SBA-15 materials were also efficient in catalyzing the reduction of 4-NP to 4-AP. The high surface area, pore symmetry and benign nature of the SBA-15 materials make it a suitable support for metal nanoparticle loading and make it a good candidate for catalytic applications.

Acknowledgement

The author gratefully acknowledges the services obtained from JNCASR Bangalore and IASST Assam for XRD; SAIF NEHU, Shillong for TEM and to GU for UV and other facility. This work is part of Ph.D. thesis of N. Kalita.

References

[1] Timofeeva, M. N; Jhung, S. H.; Hwang,Y. K.; Kim , D. K.; Panchenko, V. N.; Melgunov, M. S; Chesalov, Y. A.; Chang, J. S. *Applied Catalysis A: General*, **2007**. 317, 1, 1.

[2] Taghavimoghaddam, J. ; Knowles, G. P. ; Chaffee, A. L. *J. of Molecular Catalysis A: Chemical*, **2013**, 379, 277.

[3] Liu, G.; Liu, M,; Sun, Y, ; Wang, J, ; Sun, C, ; Li, H. *Tetrahedron: Asymmetry*, **2009**, 20, 2, 240.

[4] Dinse, A. ; Khennache, S. ; Frank, B.; Hess, C. ; Herbert, R. ; Wrabetz, S. ; Schlögl, R. ; Schomäcker, R. *J. of Molecular Catalysis A: Chemical*, **2009**, 307, 1–2, 43.

[5] Khan, N. A.; Hasan, Z. ; Jhung, S. H. *J. of Hazardous Materials*, **2013,** 244 , 444.

[6] Da'na, E. ; Sayari, A.; *Chemical Engineering Journal*, **2011,** 166, 1, 445.

[7] Saha, D. ; Warren, K. E. ; Naskar, A. K. *Carbon*, **2014.** 1, 1.

[8] Sathish Kumar, K .; Jaikumar, V. *Iranian Journal of pharmaceutical research :* **2011**. 10, 3, 415.

[9] Wang, H. ; Liu, C. J. *Applied Catalysis*

B: Environmental, **2011.** 106, 3–4, 672.

[10] Lin, D. H. ; Jiang, Y. X.; Wang, Y. Sun, S. G. *J. of Nanomaterials*, **2008.** 1

[11] Li, Y. ; Li, N. ;Tu, J. ; Li, X. ; Wang, B. ; Chi, Y. ; Liu, D. ; Yang, D. *Materials Research Bulletin*, **2011**, 46, 12, 2317.

[12] Baatz, C. ; Prüße, U. *J. of Ca talysis*, **2007**, 249, 1, 34.

[13] Carrero, A. ; Calles, J. A. ; Vizcaíno, A. J. *Applied Catalysis A: General*, **2007,** 327, 1, 82.

[14] Han, P .; Wang, X. ;Qiu, X. ; X. Ji, X. ; Gao, L. *J. of Molecular Catalysis A: Chemical*, **2007**, 272, 1–2, 136.

[15] Zhao, D. ; Feng, J. ; Huo, Q. ;. Melosh N. ; Fredrickson, G. ; Chmelka, B. ; Stucky, G. *Science* **1998**, 279, 548.

[16] Luan, Z.; Maes, E. M. ; Heide, P. A. W. van der. ; Zhao, D.; Czernuszewicz, R. S.; Kevan, L. *Chemistry of Materials*, **1999,** 11, 12. 3680.

[17] Ungureanu, A. ; Dragoi, B. ; Chirieac, A. ; Ciotonea, C.; Royer, S. ; Duprez, D. ; Mamede, A. S. ; Dumitriu, E. *ACS Applied materials & interfaces*, **2013**, 5, 8, 3010.

[18] Wang, L.; He, H.; Zhang, C. ; Sun, L. ; Liu, S.; Yue, R. *J. of applied microbiology*, **2014,** 116, 5, 1106 .

[19] Barrett, E. P. ; Joyner, L. G. ; Halenda, P. P. *J. of the American Chemical Society*, **1951**, 73, 1948, 373

[20] Pozun, Z. D, ; Rodenbusch, S. E. ; Keller, E.; Tran, K. ; Tang, W. ; Stevenson, K. J. ; Henkelman, G. *J. of physical chemistry. C, Nanomaterials and interfaces*, **2013,** 117, 15, 7598.

[21] Yang, L. ; Qi, Y. ; Yuan, X. ; Shen, J. ; Kim, J. *J. of Molecular Catalysis A: Chemical*, **2005**, 229, 1–2, 199.

[22] Cho, Y. S. ; Park,J. C. ; Lee, B. ; Kim, Y. ; Yi, J. *Catalysis Letters*, **2002,** 81, 1–2, 89.

[23] Barrón Cruz, A. E. ; Melo Banda, J. A. ; Mendoza, H. ; Ramos-Galvan, C. E. ; Meraz Melo, M. A.; Esquivel, D. *Catalysis Today*, **2011,** 166, 1, 111.

[24] Leofanti, G.; Padovan, M.; Tozzola, G. Venturelli, B. *Catalysis Today*, **1998**, 41, 1–3, 207.

[25] Meynen, V. ; Cool, P. ; Vansant, E. F. *Microporous and Mesoporous Materials*, **2009**, 125, 3, 170.

[26] de Boer, J. H. ; Lippens,B. C. ; Linsen, B. G.; Broekhoff, J. C. P. ; van den Heuvel, A. ; Osinga, T. J. *J. of colloid and interface science*, **1966,** 414, 405

[27] Harkins, W. D. ; Jura, G. *J. of American Chemical Society*, **1944,** 309, 1, 1366.

[28] Barrett, E. P.; Joyner, L. G.; Halenda, P. P. *J. of the American Chemical Society*, **1951.** 73, 1, 373.

[29] Lowell, S. ; Shields, J. E. ; Lowell, S. ; Shields, J. E. *Powder Surface Area and Porosity*, 2nd Ed. Chapman and Hall Ltd, **1984**.

[30] Zhang, Z. ; Shao, C.; Sun, Y. ; Mu, J. ; Zhang, M. ; Zhang, P. ; Guo, Z. ; Liang, P. ; Wang, C. ; Liu, Y. *J. of Materials Chemistry*, **2012**, 22, 4, 1387.

[31] Baxter, R. J. ; Hu, P. *The J. of Chemical Physics*, **2002**, 116, 11, 4379.

[32] Kalekar, A. M. ;Sharma, K. K. K. ; Lehoux, A. ; Audonnet, F. ;Remita, H. ; Saha, A. ; Sharma, G. K. *Langmuir, **2013**,* 29, 36,11431.

[33] Mahmoud, M. A. ; Poncheri, A. ; Badr, Y. ; Abd El Waned, M. G. *South African J. of Science*, 2009. 105, 7–8, 299.